Jurnal Teknologi

Full Paper

APTES AND TEOS MODIFIED BINARY RECYCLABLE HYBRID Fe_3O_4@GO NANOCOMPOSITE FOR PHOTOCATALYTIC DYE REMOVAL

Ghani Ur Rahman, A. F. Ismail*, P. S. Goh, M. Rezaei-Dasht Arzhandi, N. Ismail

Advanced Membrane Technology Research Center (AMTEC), Universiti Teknologi Malaysia, 81310 UTM Johor Bahru, Johor, Malaysia

Article history
Received
1 August 2017
Received in revised form
5 February 2018
Accepted
15 February 2018
Published online
3 June 2018

*Corresponding author
afauzi@utm.my

Graphical abstract

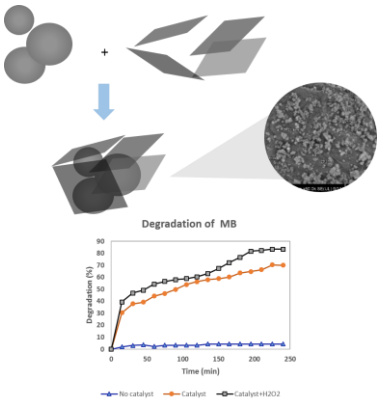

Abstract

Methylene blue (MB) is one of the industrial used organic dye and recalcitrant pollutant which creates a serious water pollution. Among the available techniques, photo degradation using light irradiation is one of the desirable choice to treat waste water. In this regard, we synthesized a binary nanocomposite of magnetite decorated with graphene oxide sheet (Fe_3O_4@GO) with modification of tetraethyl orthosilicate (TEOS) and 3-Aminopropyl triethoxysilane (APTES) by mechanical stirring method. The prepared nanocomposite was tested as a potential heterogeneous catalyst for degradation of methylene blue (MB) under UV irradiation. The synthesized nanoparticles were characterized by using X-ray diffraction (XRD), Field Emission Scanning Electron Microscopy (FESEM), Fourier transform infrared (FTIR), Thermogravimetric Analysis (TGA), and Energy-dispersive X-ray spectroscopy (EDX) techniques. The characterizations confirm the successful synthesis of the nanocomposite. The photocatalytic activity of the catalysts was gradually enhanced with time intervals. The maximum MB removal efficiency of 70.06 % was achieved over Fe_3O_4@GO composite catalyst, remarkably higher than using pure Fe_3O_4 (57.56 %). The newly developed materials was successfully recovered using an external magnet.

Keywords: Binary nanocomposite, Fe_3O_4@GO, APTES and TEOS, methylene blue (MB)

Abstrak

Metilene biru merupakan salah satu pewarna organik industri dan sukar dihapuskan menyebabkan masalah pencemaran air yang serius. Antara pelbagai teknik yang ada, sinaran fotodegradasi adalah salah satu pilihan yang paling dikehendaki untuk merawat air kumbahan ini. Di sini, kami mensintesis nano komposit binary magnetit baharu yang dihiasi dengan lapisan grafinoksida (Fe_3O_4@GO) dengan pengubahsuaian APTES dan TEOS melalui kaedah pengacauan mekanikal. Nanokomposit yang disediakan telah digunakan sebagai pemangkin heterogeneous yang efektif berpotensi untuk degradasi pencemar metilene biru (MB di bawah sinaran UV. Nanopartikel yang disintesis telah dicirikan menggunakan pembelauan sinar-X (XRD), mikroskopi imbasan electron pancaran medan (FESEM), spektroskopi infra merah jelmaan Fourier (FTIR), analisis termogravimetri (TGA), dan teknik spekro skopisinar –X penyebaran tenaga (EDX). Pencirian-pencirian tersebut mengesahkan sintesis nano komposit yang berjaya. Aktiviti pemangkinan foto nano komposit pemangkin foto tersebut adalah 70.06% iaitu lebih tinggi daripada 57.56% Fe_3O_4 tulen. Pemangkin foto yang baru dibangunkan boleh didapatkan semula dengan jayanya menggunakan sebuah magnet luar.

Kata kunci: Komposite nano Binari, Fe_3O_4@GO, APTES and TEOS, methylene blue (MB)

1.0 INTRODUCTION

Water pollution is one of the main hazards and challenges that human beings are facing today. Dyes are among these organic pollutants, which change the environmental water quality [1]. Dyes wastewater which is discharged from several industries like textiles, printing, food and cosmetics and has developed a key hazard to human and ecosystem due to the toxicity and non-biodegradability [2, 3]. For the removal of dye from the water, several conventional processes are used, but they have high operating cost, low removal efficiency and slow procedures and at higher concentrations of the organic pollutants in particular, they possess some complications during operation [4]. Photo-degradation is a promising method for the treatment of toxic and bio-resistant pollutants, and this process has some advantages on the other opposing methods. These are: (i) No secondary pollution production, (ii) complete mineralization, (iii) only mild temperature and pressure conditions are necessary and (iv) low cost [5]. Some of the semiconductors, which have been produced and studied as photocatalysts contain ZnO, TiO_2, $SrTiO_3$, Fe_2O_3, CdS, WO_3, ZnS, $FeTiO_3$, ZrO_2, V_2O_5, Nb_2O_5, SnO_2 and so on [6, 7]. These photocatalysts demonstrate positive catalytic activity along with better applicability, however, the timely separation of photocatalysts from the purified aqueous solutions sometimes becomes a challenging problem. If the already used catalysts cannot be totally recovered, then the secondary pollution may get activated via the residual photocatalyst powder [8, 9]. What is more, recyclability is similarly a new vital feature for a photocatalyst because it can exceptionally improve the cost-benefit.

To overcome the aforementioned problem magnetite (Fe_3O_4) nanoparticles (NPs) are used as photocatalyst which are eco-friendly nanomaterial, which exhibit characteristics like magnetic separation, easy recovery, and enhancement decent magnetic, electric, catalytic properties and biocompatibility [10]. Fe_3O_4 have large surface to volume ratio and have high surface energies. Redistribution and changing coordination situation of charge and atoms at the surfaces of nanoparticles intensely effects their reactivity. Furthermore, covalently bound surfactants avoid aggregation and increase dispersion stability of nanoparticles by increasing surface charge and electrostatic repulsion or by reducing interfacial energy between particle and solvent [11]. Beside, this coulombic attractions, hydrophobic interactions, and surfactant concentration affect the adsorbed surfactant mass and layer conformation and hence the ability of a surfactant to stabilize a nanoparticles against aggregation [12]. The average size of the prepared nanoparticles ranging from 50 to 200 nm and high magnetic saturation value (Ms = 48.6 emu/g) and might be used as MRI distinction agents (r^2 = 36.3 s^{-1} mM^{-1}) [13]. Moreover, Fe_3O_4 has magnetic moments for an 8-nm dot and 53-, 93-, and 174-nm single clusters of 8.45×10^{-17}, 3.23×10^{-14}, 1.79×10^{-13}, and 7.13×10^{-13} emu, respectively [14]. The super-paramagnetic characteristics of Fe_3O_4 tolerate separation under low magnetic fields to allow recycling and reuse. Furthermore, the naked Fe_3O_4 NPs have high chemical activity, and are simply oxidized in air, mostly causing in loss of magnetism and dispersibility [15]. Consequently, if proper surface coating and developing some active protection approaches to possess the stability of magnetic iron oxide NPs is very significant. Practically, it is worthy that in many cases the protecting shells not only stabilizes the magnetic iron oxide NPs, but can also be used for further functionalization [16]. Furthermore, Fe_3O_4 has outstanding conductivity, so it might perform as an electron transfer channel and acceptor, which might destroy the photo-generated carrier recombination. But, because of strong magnetic dipole-dipole attractions between particles, the magnetic Fe_3O_4 NPs tend to aggregate seriously, which greatly limits their application. To overcome this problem of aggregation the researcher start thinking about the hybrid system of Fe_3O_4. So far, a great number of semiconductors such as MnO_2, CdS, SiO_2, TiO_2, and g-C_3N_4, loaded on the surface of Fe_3O_4 have been investigated to design visible-light-driven composite photocatalysts [17, 18]. These hybrid NPs photocatalytic system strategy must fulfil the following necessities: facile preparation and synthesis method, high photocatalytic capacity, can be recycled by external magnetic fields and possess excellent photo decomposition resistance capacity [19].

One more active method for enhancing the performance of hybrid Fe_3O_4 NPs photocatalyst is the use of carbon materials as a composite which shows an active electron transfer reactions. In this consequence, two-dimensional carbon materials such as activated carbon, graphene-oxide (GO), graphene and graphdiyne are used as a carbon additive for the Fe_3O_4 photocatalysts [20, 21]. Moreover, graphene sheets have great consideration for developing nanohybrid materials for photocatalyst due to its excellent electrical, thermal, mechanical properties, and high theoretical surface area of up to 2630 m^2 g^{-1}. The other main capability of GO is to anchor guest molecules on its basal planes by guest-host interaction [22]. On this regards there are two component nanohybrid systems like WO_3/rGO, GO/g-C_3N_4, TiO_2/rGO and Fe_2O_3/rGO, have been developed to achieve higher photocatalytic performance [23, 24].

The Fe_3O_4 hybrid have other various deficiencies like leaching under acidic conditions, being disposed to autoxidation and toxicity. Moreover, uncovered Fe_3O_4 nanoparticles can easily be oxidized under severe extraction situations and lose their magnetism at long-term use. Thus, shelter of the surface of the nanocomposite can be done to moderate these adverse features [25]. For this reason, Fe_3O_4 are

surrounded in a polymeric, hybrid or inorganic matrix. The surface of the Fe_3O_4 NPs can be modified by different functional groups. Among these diverse functional groups, the amino groups have bi-functional nature that could remove cationic and anionic pollutants from aqueous media. At low pH values, the protonated amino groups adsorb anionic pollutant by electrostatic attraction, while at higher pH, amino group is used for the removal of cationic pollutants such as heavy metal ions [26]. Tetraethyl orthosilicate (TEOS) and 3-Aminopropyl triethoxysilane (APTES) are the most commonly used functional groups to produced amino-functionalization of silica-based materials [27, 28]. The use of TEOS round the magnetic NPs increases their stability in solution, avoiding or reducing the formation of agglomerates because of magnetic dipole–magnetic dipole interactions. Moreover, TEOS materials are mostly used for functionalization, because of its availability, cheapness, high stability, biocompatibility and flexibility in surface modification [29]. TEOS also help in the formation of a covalent bond between a molecule attached on the GO surface and that of Fe_3O_4 nanoparticles [30]. APTES can provide a rich NH_2 group on the surface of Fe_3O_4 nanoparticles and form hydrogen bonds with functional group present on the GO surface. Furthermore, APTES is normally used to stabilize Fe_3O_4 nanoparticles and to introduce amine groups for successive chemical functionalization [31, 32]. Based on these characteristics in many studies TEOS and APTES are used for the surface modifications of nanoparticles.

Herein, we report the preparation of Fe_3O_4@GO NPs modified by APTES and TEOS nanoparticles. The photocatalytic activities of the hybrid nanocomposite were assessed via the degradation of MB as a model reaction. It is found that Fe_3O_4@GO sphere nanoparticles show excellent photocatalytic activity for degrading of MB in comparison without catalyst. The high photocatalytic activity was endorsed to the high concentration of oxygen vacancies of GO and the existence of Fe^{+3}ions in the core/shell catalyst.

2.0 METHODOLOGY

2.1 Materials

Graphite powder, H_2SO_4, $NaNO_3$, NaOH, H_2O_2 (30%), and $KMnO_4$ were purchased from Sigma-Aldrich (USA). Iron (II) sulphate heptahydrate ($FeSO_4 \cdot 7H_2O$, 98%, M.wt = 151.91 g·mol^{-1}), sodium nitrite ($NaNO_3$, 99%), methylene blue (MB), were purchased from Sigma-Aldrich (Nottingham, UK). Isopropyl alcohol concentrated ammonium aqueous solution ($NH_3 \bullet H_2O$ 25 wt %) was purchased from Merck KGaA Germany. Ethanol, (99.9%) was purchased from RCI Labscan. TEOS (98%) was purchased from ACROS, APTES was purchased from New Jersey USA, and Acetone was purchased from RCI Labscan Limited. $BaCl_2$ was purchased from sigma-Adrch. All the chemicals were used without any further purification, and solutions were prepared using distilled water and used for all the preparations.

2.2 Synthesis of Magnetic Fe_3O_4 Nanoparticles

Fe_3O_4 nanoparticles were prepared by dissolving 3.3 g of $FeSO_4 \cdot 7H_2O$ and 2 g of $NaNO_3$ in 50 mL of distilled water. After that, 20 mL of NaOH solution (2.5 M) was poured into the mixture as it was heated up to 80˚C. The reaction was proceed at 80˚C under constant stirring to confirm the complete growth of the nanoparticle crystals. After 30 minutes, the resulting suspension was cooled down to room temperature and washed with distilled water repeatedly to remove unreacted chemicals. The magnetic Fe_3O_4 nanoparticles were separated by using an external magnet and dried in an oven at 60˚C overnight before coating.

2.3 Synthesis of GO from Grapite Powder Using Modified Hummers' Method

In brief, GO was prepared by the oxidation of graphite using $KMnO_4$ as a strong oxidizing agent. 3 g of graphite and 1.5 g of $NaNO_3$ was mixed well in 69 mL of concentrated H_2SO_4. The mixture was cooled to 0°C using ice bath and stirred for 15 min. Then 9 g of $KMnO_4$ was added slowly into the mixture while maintaining the temperature below 20 °C to prevent overheating and explosion. After stirring for 2 hr the ice bath was replaced by water bath and the mixture was then stirred vigorously for another 30 min at 35 °C. RO water (150 mL) was added and the temperature of the mixture was maintained below 95°C for 15 min of stirring. Finally, the reaction was terminated by addition of RO water (500 mL) and 30% H_2O_2 solution (15 mL) to reduce the residual permanganate and manganese dioxide to colourless soluble manganese sulphate. The resulting mixture was filtered, and then filtered graphene oxide was washed with 5% HCl aqueous solution until sulphate could not be detected by $BaCl_2$. The GO was then washed by RO water and centrifuged until the supernatant reaches pH 5 to 6. Then the GO solution was ultrasonicated for 1hr and the GO mud was obtain by centrifuging at 4000 rpm for 2 hours to remove large and not fully exfoliated GO. The GO was dry in vacuum oven at 60 °C for 12 hrs. To further purify the GO, the dried GO was dissolved back into large amount of acetone and was stirred vigorously. At last, the GO solution was filtered and the obtained GO cake was dry in vacuum oven again at 60 °C for 6 hrs.

2.4 Preparation of Fe_3O_4@GO Nanospheres

To synthesis magnetic Fe_3O_4@GO nanocomposite, the surface of Fe_3O_4 was first modified with APTES that supplies amide group for more binding graphene oxide by the electrostatic action. 0.1 g of Fe_3O_4

particles were mixed of ethanol (80 mL), deionized water (20 mL) and concentrated ammonia aqueous solution (1.0 mL, 28 wt. %) under ultrasonication, followed by the addition of 67 µL of TEOS and 67 µL of APTES. After stirring at 35℃ for 3 h, the Fe_3O_4 spheres were functionalized with amino groups (Fe_3O_4@NH_2). The prepared nanocomposite was separated and washed with ethanol and water by an external magnetic field. The binary hybrid of Fe_3O_4@NH_2 were redispersed in the GO aqueous solution (1.0 mg/mL) to synthesize the magnetic graphene (Fe_3O_4@GO) under vigorous stirring at 75°C for 1 h. In direction to eliminate the remaining GO, the achieved Fe_3O_4@GO particles were washed with deionized water for 3 times.

2.5 Instrumentation

A structural details of the samples were studied by X-ray diffraction (XRD) (D8 Advance Diffractometer, Bruker, USA) using CueKa radiation (0.154 nm) at 40 kV and 100mA. The field-emission scanning electron microscope (FESEM, JEOLJSM 6380LA) attached with energy dispersive X-ray spectroscopy (EDX) were employed for observing layer formation and elemental analysis. The FTIR spectra of all the compounds were recorded in potassium bromide disks using a Perkin Elmer 2000 system spectrometer in the range 4000-400 cm^{-1}. Thermo gravimetric analysis (TGA) has been carried out (Metler-Toledo) in air (flow rate) 50 mL/min) in the temperature range 30-1000 °C (heating rate) 5 °C/min).

2.6 Photocatalysis Experiments

The photocatalytic activity of the as-prepared composite nanospheres was calculated by photodegradation of MB in aqueous solution under UV. All catalytic reactions were conducted in a 1000 mL radius flask with constant mechanical stirring at room temperature. For the degradation of MB, desired amount of the as-prepared catalysts was added into the 1000 mL aqueous solution containing 20 mg/L MB. The suspension with the photocatalyst but without any H_2O_2 was stirred for 90 min to reach adsorption-desorption equilibrium between the catalysts and MB so that the adsorption in the dark can be discounted. The lamp was turned on while a 0.186 M of H_2O_2 was adding to the mixed solution. During the reaction, 10 mL of sample was withdrawn at each time interval (15 min) and filtered using a syringe filter (Millex PES, 0.22 µm) and the catalysts were collected by magnetic separation. The disappearance of MB was spectrometrically observed as a function of irradiation time using a UV-Vis spectrophotometer at a wavelength 664 nm. The photocatalytic degradation rate and elimination efficiency of MB under UV radiation were calculated by measuring the absorbance of collected solutions by UV-vis spectrophotometer at λ_{max} 664 nm, which is usually determined by

$$\% \text{ degradation} = \frac{(C_o - Ce)}{C_o} \text{ x100}$$

Where, C_o is the initial concentration of MB and C_e is the concentration of MB at time t during the catalytic reaction respectively.

3.0 RESULTS AND DISCUSSION

3.1 FTIR Analysis

The nanocomposite was studied by FTIR analysis. The main peaks of GO at 3515, 1430, 1630, 1230 and 1080 cm^{-1} confirm the presence of hydroxyl, carboxyl and epoxide groups on the GO sheets as shown in Figure 1 (A). The transmission infrared spectra of Fe_3O_4@GO of the synthesized products are shown in Figure 1 (B). The strong signal at 576cm^{-1} is consigned to the Fe-O stretching vibration. In the FT-IR spectrum of the Fe_3O_4@GO, the bands detected in the region of 1400-1600 cm^{-1} and 1200-1400 cm^{-1} are the characteristic vibrations of C=N and C–N heterocycles bonds, correspondingly. There is a weak peak at 1640 cm^{-1} which be similar to the bending vibration of –OH groups that is generally seen in Fe_3O_4 formed by the chemical co-precipitation reaction.

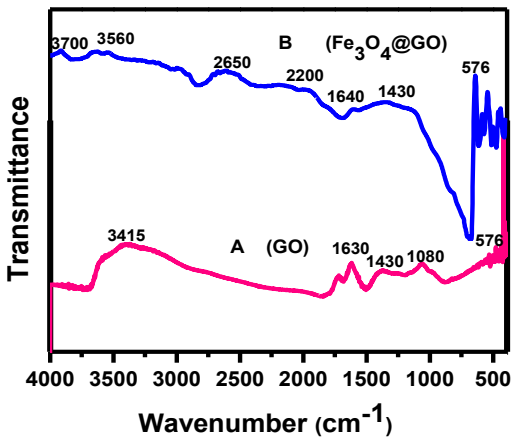

Figure 1 FTIR patterns spectra (A) for GO and (B) for Fe_3O_4@GO explanation

3.2 TGA Analaysis

The thermal stability of the synthesized samples was also confirmed by using TGA analysis as shown in Figure 2. The carbon content of the GO and GO@Fe_3O_4 composite was determined by TGA. According to the curve, GO was more thermally unstable than graphite in which it experienced a three step degradation. GO lost 12% weight up to 180 °C. The weight loss could be attributed by the evaporation of adsorbed water and thermal decompositions of oxygen-containing functional

groups like carboxyl, hydroxyl, epoxy, nitrogen dioxide, and ketone. The weight loss rate of GO increased to 34 % with increasing temperature from 180 °C to 220 °C because GO is unstable in high temperature [33]. Furthermore, there is a decrease in the loss rate to attain a maximum value about 44.57 wt. % at about 700 °C, proposing the existence of structural shortcomings in GO produced by strong acid oxidation as shown in TGA curve (A). The weight loss percentage for the Fe_3O_4@GO hybrid was examined from the curve (B), where it showed higher stability than GO in the range 12% up to 220 °C and only 35% than 44.57% at about 870 °C. The maximum weight loss 50.20 % was obtained at about 999.63 °C. From above discussion, it is clear that Fe_3O_4@GO composite is thermally more stable than GO. The combustion of carbon begin around 400 °C, and the weight change was nearly completed at about 999.63 °C. However, the mass that remained constant above 400 °C was consigned to Fe_3O_4@GO [34]. This method can represent the actual Fe_3O_4@GO content which were Fe, C and O in the complex.

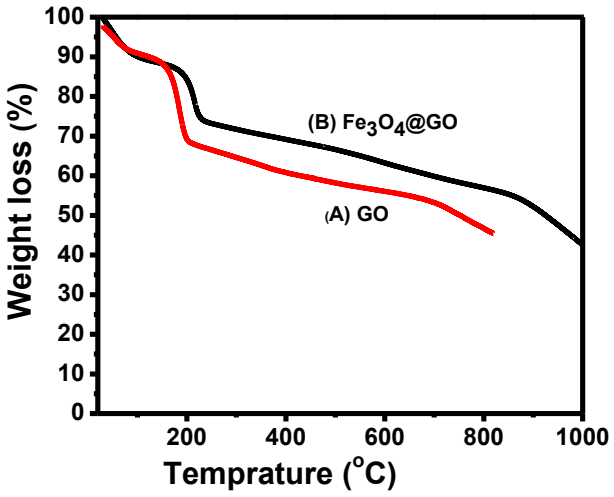

Figure 2 TGA explanation (A) for GO and (B) for Fe3O4@GO

3.3 XRD Analysis

The structure of the prepared nanocomposite was also studied by XRD analysis as shown in Figure 3. The characteristic diffraction peaks for Fe_3O_4 (2θ = 13.11°, 30°, 35.4°, 43.3°, 53.4°, 57.1° and 62.7°), which can be indexed to their indices (100), (220), (311), (400), (422), and (440), were observed for the synthesized Fe_3O_4 nanoparticles. This result corresponds well to the PDF data (JCPDS file No. 19-0629) which shows that the magnetite diffraction peaks appeared at the same locations. Besides, this result is also in good consistency with the XRD characterization of Fe_3O_4 reported in the former literature [35]. After the modification by APTES, TEOS and GO, only the concentration of the obtained nanocomposite altered, which have shown that the amount of the GO is too minute to accomplish its crystallinity. Besides that, the crystallinity of Fe_3O_4 was not significantly altered by APTES, TEOS and GO [36].

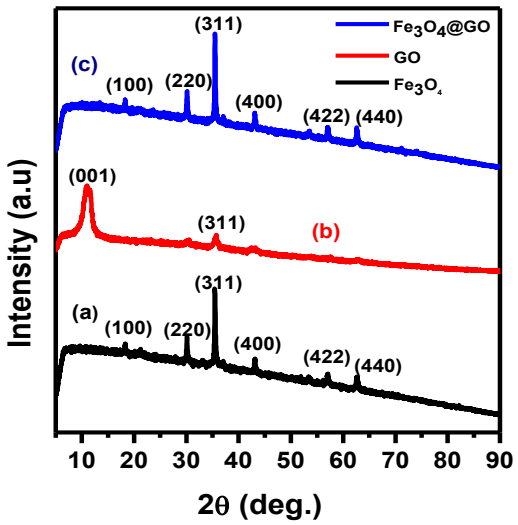

Figure 3 XRD spectrum (a) for Fe_3O_4 (b) GO and (c) Fe_3O_4@GO

3.4 FE-SEM Analysis

FE-SEM image analysis is relatively suitable for the investigation of surface morphology and particle size/shape. Figure 4(a) shows the FE-SEM image of sphere shaped Fe_3O_4 particles and the average size of the particles is in the range of 17.2-21.2 nm. These particles are non-aggregated with narrow size distribution. Figure 4(b) shows that the Fe_3O_4@GO particles immobile have the morphological properties of pure Fe_3O_4 except for a slightly larger particle size about 25.5nm to 29.0 nm, which may be due to by the coating of GO on the surface of the magnetic core. Figure 4 (b) shows that the Fe_3O_4 nanoparticles were spread on the basal planes of the graphene. From the figure, one can notice that the graphene sheets were dispersed between the loosely packed Fe_3O_4 and that of a big extent of void spaces formed on the material. Furthermore, the graphene sheets distributed between the Fe_3O_4 can avoid the aggregation of Fe_3O_4 to a certain extent, which can be of great benefit to reactions.

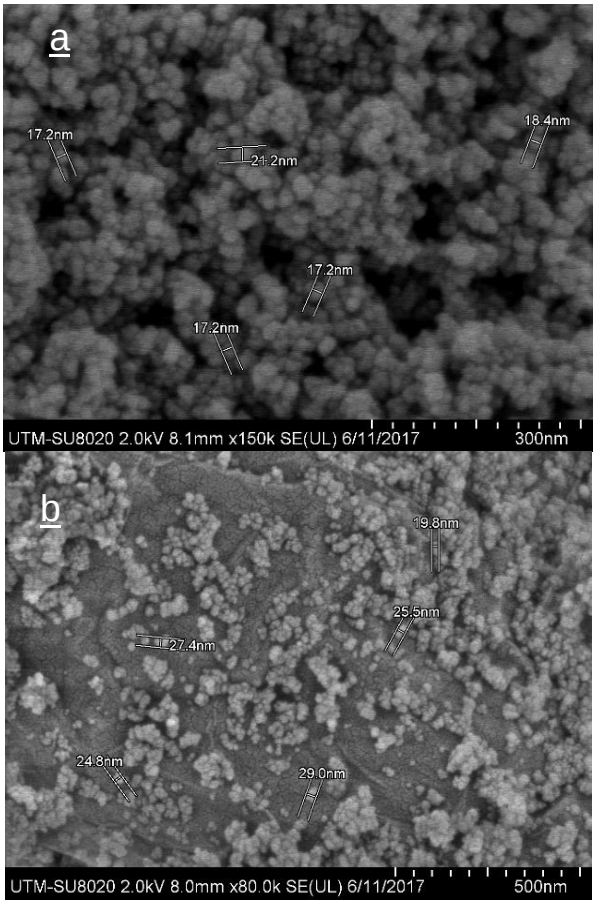

Figure 4 FESEM images for (a) Fe_3O_4 and (b) Fe_3O_4@GO

3.5 EDX Analysis

The synthesized GO and Fe_3O_4@GO particles were also characterized by the energy dispersive X-ray (EDX) spectroscopy by a casting film and the result of Figure 5 (a) show strong peaks of Fe and O. The compositions of the Fe_3O_4 by mass percent are Fe 68.9 %, O 31.1 %. The corresponding atomic composition are Fe 55.3 %, O 15.8 % and C 28.9 % as depicted in Figure 5 (b) which imply that the nanospheres is mostly consist of Fe, C and O elements. The peak which arise in both Figure 5 (a) and (b) at the position of 2.5 eV is attributed to the presence of silica in trace amount due to the modification of Fe_3O_4 by APTES and TEOS but in traces.

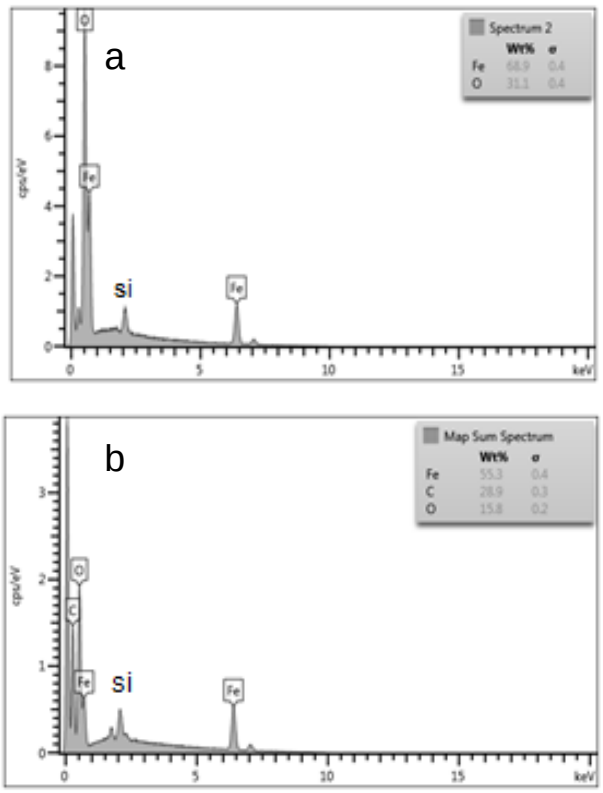

Figure 5 EDX survey spectra of Fe_3O_4 spheres (a) and Fe_3O_4@GO (b)

3.6 Photodegradation of MB BY Fe_3O_4 @GO

The photocatalytic activity of the synthesized nanocomposite for degradation of MB under UV-light radiation was studied and the results are shown in Figure 6 (the photolysis of MB (20 mg/L) under the UV light radiation lacking of photocatalyst after 240 min is less than 5%). Hence, the results showed that the photocatalyst plays a predominate role in the degradation of MB aqueous solution. For comparison, photocatalytic activity was also checked out with Fe_3O_4 and Fe_3O_4@GO nanoparticles. The photocatalytic activity of the Fe_3O_4 toward MB was 57.56 %, this results reveals that the photocatalytic performance of Fe_3O_4 under the UV-light illumination is subsequently slow. At this point, the low degradation efficiency of Fe_3O_4 can be ascribed to its large band gap as well as rapid recombination rate of charge carriers. However, after combination with GO, the photocatalytic activity of the compound photocatalysts are remarkably improved to 70.06%. It is obviously evidenced that photodegradation of MB is higher than Fe_3O_4 catalysed solution. The results implied that the presence of GO plays an important role in enhancing the performance of the Fe_3O_4. Graphene-based hybrid photocatalyst poses numerous advantages over Fe_3O_4 due to the exclusive electronic properties resulting from the sp^2

hybridized carbon atoms transaction a picosecond ultrafast electron transfer method from the excited semiconductors to the graphene sheet and the controllable size of the semiconductors and reduced aggregation of the graphene sheets promote recover the efficiency of the photocatalysis. Besides, the high transparency of the graphene sheets as of their one- or several-atoms thickness, accelerate the consumption of the exciting light given the conducting and semiconducting properties of graphene, it is probable that photoexcited electrons from Fe_3O_4 are transferred to graphene to hinder electron-hole recombination and to boost oxidative reactivity. Moreover, in incidence of UV irradiation, H_2O_2 plays dynamic role in degradation of MB as it produces two hydroxyl radicals ($HO^{\bullet}$). The $HO^{\bullet}$ are considered exceptionally robust oxidant for the degradation of organic pollutants such as MB [37]. Furthermore, the synergistic interaction between GO and Fe_3O_4 makes the electron transfer easy, which can facilitate the reduction of Fe^{3+} to Fe^{2+}as well as generation of $HO^{\bullet}$. Consequently, the combination of H_2O_2 with Fe_3O_4@GO helps in MB degradation. Therefore, the best photocatalytic performance was observed for the Fe_3O_4@GO with the addition of H_2O_2, which was nearly 83.36 % of MB molecules within the UV irradiation for 240 min as shown in Figure 6.

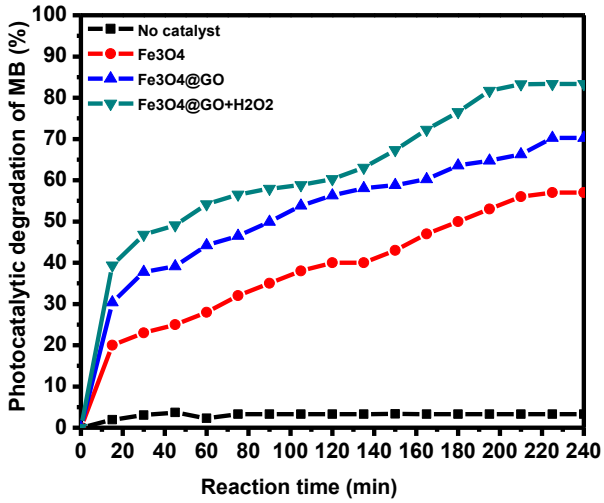

Figure 6 Photocatalytic degradation of MB in the presence of Fe_3O_4, Fe_3O_4@GO hybrids and along with H_2O_2

4.0 CONCLUSION

In this study, the presence of catalyst Fe_3O_4@GO in the photodegradation system has increased the degradation rate of Methylene blue in water. The prepared Fe_3O_4@GO structure was confirmed by characterization of FTIR spectrum, XRD, TGA, FE-SEM and EDX test techniques. The presence of catalyst in the degradation of MB dye was found to be much higher as compared to noncatalysized solution. The modification of Fe_3O_4 by APTES and TEOS proven high thermal stability as described in TGA analysis. The comparison of mono and binary nanocomposite and along with H_2O_2 shown consistency in degradation rate. The high degradation of MB was up to 83.36 % in the presence of H_2O_2 within four hours, which indicates that the system has the potential to be operated in a larger scale.

Acknowledgements

This work was supported by Universiti Teknologi Malaysia under Research University Grant (13H65) Special Flagship Research Grant (02G07).

References

[1] Rajeshwara, K., Osugib, M. E., Chanmaneec, W., Chenthamarakshana, C. R. Zanonib, M. V. B., Kajitvichyanukuld, P. and Krishnan, -A. 2008. R. Heterogeneous Photocatalytic Treatment of Organic Dyes in Air and Aqueous Media. *Journal of Photochemistry and Photobiology C: Photochemistry Reviews*. 9: 171-192.

[2] Chen, Y. Z., Li, N., Zhang, Y. and Zhang, L. D. 2014. Novel Low-cost Fenton-like Layered Fe-titanate Catalyst: Preparation, Characterization and Application for Degradation of Organic Colorants. *Journal of Colloid. Interface. Science*. 422: 9-15.

[3] Lin, Y. *et al.* 2012. Ternary Graphene-TiO2-Fe3O4 Nanocomposite as a Recollectable Photocatalyst with Enhanced Durability. *European Journal of Inorganic Chemistry*. 28: 4439-4444.

[4] Ke, D., Tianyou, P., Dingning, K. and Bingqing, W. 2009. Photocatalytic Hydrogen Generation using a Nanocomposite of Multi-walled Carbon Nanotubes and TiO2 Nanoparticles under Visible Light Irradiation. *Nanotechnology*. 20: 125603-125608.

[5] Shouhu, X., Wanquan, J., Xinglong, G., Yuan, H. and Zuyao, C. 2009. Magnetically Separable Fe_3O_4/TiO_2 Hollow Spheres: Fabrication and Photocatalytic Activity. *Journal of Physical Chemistry C*. 113: 553-558.

[6] Andrew, M. and Stephen, L. H. 1997. An Overview of Semiconductor Photocatalysis. Elsevier. *Journal of Photochemistry and Photobiology A: Chemistry*. 1(108): 1-35.

[7] Rehman, S., Ullah, R., Butt, A. M. and Gohar, N. D. 2009.Strategies of Making TiO_2 and ZnO Visible Light Active. – NCB. *Journal of Hazardous Materials*. 2-3 (170): 560-569.

[8] Shouhu, X., Wanquan, J., Yufeng, Z., Yanli, Z. and Xinglong, G. 2012. Super Paramagnetic Ag@Fe_3O_4 Core–Shell Nanospheres: Fabrication, Characterization and Aapplication as Reusable Nanocatalysts. *Dalton Transactions*. 41(15):4594-601.

[9] Linley S, Leshuk T. and Gu, F. X. 2013. Magnetically Separable Water Treatment Technologies and their Role in Future Advanced Water Treatment: A Patent Review. *Clean-Soil Air Water*. 12 (41): 1152-6.

[10] Xiaohui, F., Haijuan, G., Kunal, P., Hong, Z. and Xia, L. 2014. High Performance, Recoverable Fe_3O_4-ZnO Nanoparticles for Enhanced Photocatalytic Degradation of Phenol. *Chemical Engineering Journal*. 244: 327-334.

[11] Buffl e, J., Z. Zhang, and K. Startchev. 2007. Metal Flux and Dynamic Speciation at (Bio) Interfaces. Part I: Critical Evaluation and Compilation of Physicochemical Parameters for Complexes with Simple Ligands and Fulvic/Humic Substances. *Environ. Sci. Technol.* 41: 7609-7620.

[12] Vaisman, L., H.D. Wagner, and G. Marom. 2006. The Role of Surfactants in Dispersion of Carbon Nanotubes. *Adv. Colloid Interface Sci.* 130: 37-46.
[13] Shouhu, X., Feng, W., Josie, M. Y. Lai., Kathy, W. Y. S., Yi-Xiang, J. W., Siu-Fung, L., Jimmy, C. Yu., Christopher, H. K. C., and Ken, C.-F. L. 2011. Synthesis of Biocompatible, Mesoporous Fe3O4 Nano/Microspheres with Large Surface Area for Magnetic Resonance Imaging and Therapeutic Applications. *ACS Appl. Mater. Interfaces*. 3: 237-244.
[14] Jianping, G., Yongxing, H., Maurizio, B., Ward, P. B., and Yadong, Y. 2007. Superparamagnetic Magnetite Colloidal Nanocrystal Clusters. *Angew. Chem. Int. Ed.* 46: 4342-4345.
[15] Zhang, Y., Zhao, Z. Y., Chen, J. R., Cheng, L., Chang, J., Sheng, W.C., Hu, C.Y. and Cao, S. S. 2015. C-doped Hollow TiO_2 Spheres: in Situ Synthesis, Controlled Shell Thickness, and Superior Visible-light Photocatalytic Activity. *Applied Catalysis B: Environmental*. 165: 715-722.
[16] Kim, C. H., Kim, B. H. and Yang, K. S. 2012. TiO_2 Nanoparticles Loaded on Graphene/Carbon Composite Nanofibers by Electrospinning for Increased Photocatalysis. *Carbon.* 7 (50): 2472-2481.
[17] Tarek A. Gad, -A., Shigeru, K., Shigeo, S. and Toshinori, K. 2009. Treatment of Synthetic dyes Wastewater Utilizing a Magnetically Separable Photocatalyst (TiO_2/SiO_2/Fe_3O_4): Parametric and Kinetic Studies. *Desalination*. 1-3 (244): 1-11.
[18] Dan, W., Hongmin, M., Yong, Z., Hongying, J., Tao, Y. and Qin, W. 2015. Corallite-like Magnetic Fe_3O_4@MnO_2@Pt Nanocomposites as Multiple Signal Amplifiers for the Detection of Carcinoembryonic Antigen. ACS *Appl Mater Interfaces.* 7 (33): 18786-93.
[19] Feng, L., Junjie, L., David, G. E. and Xue, D. 2004. Stoichiometric Synthesis of Pure MFe_2O_4 (M = Mg, Co, and Ni) Spinel Ferrites from Tailored Layered Double Hydroxide (Hydrotalcite-Like) Precursors. *Chemistry of Material*. 16(8): 1597-1602.
[20] Eman, A. 2017. Photodegradation of Binary Azo Dyes Using Core-Shell Fe_3O_4/SiO_2/TiO_2 Nanospheres. *American Journal of Analytical Chemistry.* 8: 95-115.
[21] Yitao, Z., Guangyu, H., Wen, D. and Haiqun, C. 2014. High Catalytic Activity in the Phenol Hydroxylation of Magnetically Separable $CuFe_2O_4$-reduced Graphene Oxide. *Industrial & Engineering Chemistry Research*. 53: 12566-12574.
[22] Veerasubramani, G. K., Krishnamoorthy, K. and Kim, S. J. 2015. Electrochemical Performance of an Asymmetric Supercapacitor based on Graphene and Cobalt Molybdate. Electrodes. *RSC Advances*. 5: 16319-16327.
[23] Kai, D., Luhua, L., Qi, L., Guangping, Z., Xiaoqin, W., Jin, B., Lingling, X. and Heng W. 2014. Sonication Assisted Preparation of Graphene Oxide/ graphitic-C_3N_4 Nanosheet Hybrid with Reinforced Photocurrent for Photocatalyst Applications. *Dalton Trans*. 43: 6295-6299.
[24] Cao1, L. L., Yin, S. M., Liang Y. B., Zhu, J. M., Fang, C. and Chen, Z. C. 2015. Preparation and Characterisation of Magnetic Fe_3O_4/Graphene Oxide Nanocomposites. *Materials Research Innovations*. 19: 364-368.
[25] Wenjun, J., Quan, C., Wei, X., Mingwei. Y., Yong, C., Dionysios, D. D. and Kevin, E. O'. 2014. Cr (VI) Adsorption and Reduction by Humic Acid Coated on Magnetite. *Environ. Sci. Technol.* 48: 8078-8085.
[26] José, A., Jesús, M. A., Amaya, A., Monta˜na, L. and Victoria, G. 2009. Aqueous Heavy Metals Removal by Adsorption on Amine-functionalized Mesoporous Silica. *J. Hazard. Mater*. 163: 213-221.
[27] Mojun, Z., Maria, Z. Lerum. and Wei, C. 2011. How to Prepare Reproducible, Homogeneous, Andhydrolytically Stable Aminosilane-Derived Layers on Silica. *Langmuir.* 28: 416-423.
[28] Robert, G. A., Amanda, V. E., Jason, A., Claire, E. L., Dmitriy, A. K., Gregory, F. M. and Gunther, G. A. 2012. Molecular Structure of 3-Aminopropyltriethoxysilane Layers Formed on Silanol-Terminated Silicon Surfaces. *J. Phys. Chem. C.* 116: 6289-6297.
[29] Fuan, H., Jintu. F., Dong, M., Liming, Z., Chiwah, L., Helen, L. C. 2010. The Attachment of Fe_3O_4 Nanoparticles to Graphene Oxide by Covalent Bonding. *CARBON.* 48: 3139 –3144.
[30] Silvia, V., Paola, R., Federico, L., and Fabio, C. 2016. Functionalization of Fe_3O_4 NPs by Silanization: Use of Amine (APTES) and Thiol (MPTMS) Silanes and Their Physical Characterization. *Materials*. 9: 826-840.
[31] Miaomiao, Y., Huihui, Z., Tuqiao, Z., Yiping, Z. and Yu, S. 2013. Preparation of SiO_2@Au@TiO_2 Core–shell Nanostructures and Their Photocatalytic Activities Under Visible Light Irradiation. *J. Chem. Engin*. 226: 209-216.
[32] Weiwei, Z. B. C., Hongxia, P., Hongjin, Q., and Yaoyu, W. C. 2015. Novel Method to Investigate the Interaction Force between Etoposide and APTES-Functionalized Fe_3O_4@nSiO_2@mSiO_2 Nanocarrier for Drug Loading and Release Processes. *J. Phys. Chem. C.* 119. 8: 4379-4386.
[33] Mithilesh, Y., Kyong, Y. R., Soo, J. P. and David, H. 2014. Mechanical Properties of Fe3O4/GO/chitosan Composites. *Composites: Part B.* 66: 89-96.
[34] Yucheng, D., Ruguang, M., Mingjun, H., Hua, C., Qingdan, Y., Yang, Y. L. and Juan A. Z. 2013. Thermal Evaporation-induced Anhydrous Synthesis of Fe_3O_4–graphene Composite with Enhanced rate Performance and Cyclic Stability for Lithium ion Batteries. *Phys. Chem. Chem. Phys.* 15: 7174-7181.
[35] Chunhui, L., Ruixue, W., Yanmin, X., Ailing, S., and Liuhe, W. 2014. Synthesis of Hexagonal and Triangular Fe_3O_4Nanosheets via Seed-mediated Solvothermal Growth. *Nano Res.* 7 (4): 536-543.
[36] Sheng, Li., Ling, X., Hongbing, D., Xiaowen, S., Qihua, C. 2017. Remote Controlled Drug Release from Multi-functional Fe_3O_4/GO/Chitosan Microspheres Fabricated by an Electrospray Method. Colloids and Surfaces. *B, Biointerfaces.* 16(151): 354-362.
[37] Poonam, B., Manish, K., Pankaj, C. and Kamal, K. K. 2015. Enhanced Photocatalytic Degradation of Methylene Blue and Adsorption of Arsenic (III) by Reduced Graphene Oxide (rGO)–metal Oxide (TiO_2/ Fe_3O_4) Based Nanocomposites. *RSC Adv.* 5: 73249-73260.